



# Kinetic Energy and Vorticity Perspectives of the Rapid Development of an Explosive Extratropical Cyclone Over the Northwest Pacific Ocean in February 2018

Hui Wang<sup>1\*</sup>, Mengjiao Du<sup>2</sup>, Chenghu Sun<sup>3</sup> and Bo Zhang<sup>1</sup>

<sup>1</sup>National Meteorological Center, Beijing, China, <sup>2</sup>Institute of Science and Technology, China Three Gorges Corporation, Beijing, China, <sup>3</sup>Chinese Academy of Meteorological Sciences, Beijing, China

## OPEN ACCESS

### Edited by:

Guihua Wang,  
Fudan University, China

### Reviewed by:

Jai Sukhatme,  
Indian Institute of Science (IISc), India  
Chenghai Wang,  
Lanzhou University, China  
Gang Fu,  
Ocean University of China, China  
Zhiqiang Gong,  
Beijing Climate Center (BCC), China

### \*Correspondence:

Hui Wang  
wangh1@cma.gov.cn

### Specialty section:

This article was submitted to  
Atmospheric Science,  
a section of the journal  
Frontiers in Earth Science

**Received:** 23 December 2021

**Accepted:** 21 February 2022

**Published:** 30 March 2022

### Citation:

Wang H, Du M, Sun C and Zhang B  
(2022) Kinetic Energy and Vorticity  
Perspectives of the Rapid  
Development of an Explosive  
Extratropical Cyclone Over the  
Northwest Pacific Ocean in  
February 2018.  
*Front. Earth Sci.* 10:841948.  
doi: 10.3389/feart.2022.841948

Explosive extratropical cyclones (EECs) have long been a research focus for the meteorological society as they often cause serious economic losses and casualties. However, after a long period of research, there still remain some knowledge gaps about their rapid development. In this article, we conducted the first study by using both vorticity and kinetic energy (KE) budgets simultaneously on a typical EEC, which was the strongest EEC that affected the coastal areas of China in the last 3 years, to further the understanding of the mechanisms governing its rapid enhancement in rotation and wind speed. The vorticity budget shows that the lower-level convergence-related vertical stretching and the vertical transport of vorticity acted as the most and second most favorable factors for the increase in the cyclone's cyclonic vorticity, respectively, which were different from those findings based on the Zwack–Okossi vorticity budget. In contrast, the horizontal transport of vorticity and tilting mainly decelerated the EEC's development. Energetics features governing the rapid wind enhancement of the EEC were shown for the first time. It is found that the work on the rotational wind by the pressure gradient force and the net import transport of KE by the rotational wind contributed the largest and second largest to the cyclone's increase in wind speed. In contrast, the upward transport of KE and the cyclone's displacement mainly acted in an opposite way. Analysis based on the Green's theorem and rotational wind shows that the enhancement of the EEC's rotation and wind speed were linked to each other solidly.

**Keywords:** EEC, vorticity budget, KE budget, rotation, wind speed

## INTRODUCTION

Extratropical cyclones are one of the most important systems in the mid-latitude regions, as they often cause severe weather such as torrential rainfall, strong winds, cold waves, and so on (Fu et al., 2014; Schultz et al., 2018). Of the extratropical cyclones, there are a special type, called the explosive extratropical cyclone (EEC), which deepens sharply with its central pressure decreased by at least 24 hPa (relative to 60°N) in 24 h (Sanders and Gyakum, 1980). The most severe disastrous weather tends to appear during

EECs' rapid development (Yoshida and Asuma, 2004); therefore, many previous studies conducted investigations on dynamical and thermodynamical processes governing EECs' rapid development. It is found that favorable dynamical factors for EECs' rapid development mainly contain a cyclonic vorticity advection aloft (Sanders, 1986; Macdonald and Reiter, 1988), a strong jet streak at upper level (Uccellini et al., 1984; Uccellini and Kocin, 1987), a strong baroclinic instability in the middle and lower troposphere (Bosart, 1981; Jia and Zhao, 1994; Iwao et al., 2012), and a notable tropopause folding process in the upper and middle troposphere (Rossa et al., 2000; Fu et al., 2014, 2018; Wang et al., 2017). Favorable thermodynamical factors mainly contain a warm temperature advection aloft (Hirschberg and Fritsch, 1991a, b; Lupo et al., 1992), strong latent heat release in the middle and lower troposphere (Bosart, 1981; Reed and Albright, 1986; Chen and Dell'Osso, 1987), reduced static stability in the lower troposphere (Smith and Tsou, 1988), and upward energy fluxes from the surface (Kuo et al., 1991).

As mentioned above, previous studies have deepened the understanding of EECs' evolution; however, as EECs' development can be affected by numerous factors, governing mechanisms may be quite different. Therefore, more case studies should be conducted. There are three indicators that can effectively measure an EEC: its central pressure, rotation, and wind speed (Sanders and Gyakum, 1980; Yoshida and Asuma, 2004; Fu et al., 2018). During EECs' developing stages, although their pressure and rotation (which can be reflected by the area-averaged vorticity within its central region) both enhance notably (Zwack and Okossi, 1986; Lupo et al., 1992; Parsons and Smith, 2004; Fu et al., 2018), their associated winds do not always strengthen simultaneously (Jiang et al., 2021a). For those EECs which showed rapid intensification in their rotation and wind (these cyclones usually have larger destructive force), what are the key mechanisms that govern these two processes? Is there a solid link between these two features? These two scientific questions remain unanswered.

At the end of February 2018, an EEC appeared over the Northwest Pacific Ocean. It was the strongest EEC that affected the coastal areas of China in the last 3 years. During its life span, strong winds (above 24 m/s) appeared, which caused severe cold waves and huge waves and resulted in great economic losses. In this study, we applied vorticity and kinetic energy (KE) budgets to this cyclone, so as to partly address the two scientific questions raised above. The remainder of this article is structured as follows: In **Section 2**, data and methods used in this study are provided; in **Section 3**, an overview of the event is shown; in **Section 4**, the results of vorticity and KE budgets were analyzed; and finally, a conclusion and discussion is presented in **Section 5**.

## DATA AND METHOD

This study used hourly,  $0.25^\circ \times 0.25^\circ$  ERA5 reanalysis data (Hersbach et al., 2020) provided by the European Centre for Medium-Range Weather Forecasts (ECMWF) for analyses and calculations. This dataset has a total of 37 vertical levels. In this study, the definition from Yoshida and Asuma (2004) was used to calculate the deepening rate (DR) of the EEC:

$$DR = \left[ \frac{p(t-6) - p(t+6)}{12} \right] \left[ \frac{\sin 60^\circ}{\sin(\phi(t-6) + \phi(t+6)/2)} \right] \quad (1)$$

where  $t$  is time (units: h),  $p$  is the cyclone's central sea level pressure [SLP (units: hPa)], and  $\phi$  is the latitude of the cyclone center.

In order to clarify the mechanisms governing the EEC's rapid development, two methods were used: one is the vorticity budget (Kirk, 2003; Fu et al., 2016; Jiang et al., 2021b) and the other is the KE budget (Chen et al., 1978; Fu et al., 2011). The former was used to analyze the rotation enhancement associated with the cyclone, and the latter was utilized to investigate its wind intensification. Although EECs have long been a research focus, their energetics features still remain vague. Investigation on EECs' wind enhancement in terms of energy is helpful to reach a more comprehensive understanding of their rapid development. The vorticity budget equation is as follows:

$$\frac{\partial \zeta}{\partial t} = \mathbf{k} \cdot \left( \frac{\partial \mathbf{V}_h}{\partial p} \times \nabla_h \omega \right) - \mathbf{V}_h \cdot \nabla_h \zeta - \omega \frac{\partial \zeta}{\partial p} - (\zeta + f) \nabla_h \cdot \mathbf{V}_h - \beta v + \text{RES} \quad (2)$$

where  $\zeta$  is the vertical component of the relative vorticity (vorticity for short);  $(i, j, k)$  are unit vectors pointing to the east, north, and zenith, respectively;  $\mathbf{V}_h = u\mathbf{i} + v\mathbf{j}$  denotes the horizontal velocity vector; subscript "h" stands for the horizontal component;  $p$  is pressure;  $\nabla_h = \partial\mathbf{i}/\partial x + \partial\mathbf{j}/\partial y$  is horizontal gradient operator;  $\omega$  is vertical velocity in pressure coordinate;  $f$  is Coriolis parameter; and  $\beta = \partial f/\partial y$ . The first term on the right-hand side of **Eq. 2** was defined as TIL, as it shows the tilting effect; the second and third terms were defined as HAV (representing the horizontal advection of vorticity) and VAV (denoting the vertical advection of vorticity), respectively; the fourth term was defined as STR, which stands for stretching effect associated with divergence; the fifth term was defined as APV, which represents the advection of planetary vorticity; and the last term is RES, which denotes the residual effect (mainly due to friction, subgrid processes, and calculation errors.). The sum of TIL, HAV, VAV, STR, and APV was defined as TOT, which shows the total effect of all terms on the right-hand side of **Eq. 2**.

The kinetic budget equation (Chen et al., 1978) is as follows:

$$\begin{aligned} \frac{1}{Sg} \int_{p_t}^{p_b} \iint \frac{\delta k}{\delta t} dsdp &= \frac{1}{Sg} \int_{p_t}^{p_b} \iint \mathbf{M}_h \cdot \nabla_h k dsdp - \frac{1}{Sg} \int_{p_t}^{p_b} \iint \nabla_h \cdot (\mathbf{V}_\psi k) dsdp - \\ \frac{1}{Sg} \int_{p_t}^{p_b} \iint \nabla_h \cdot (\mathbf{V}_\chi k) dsdp &- \frac{1}{Sg} \int_{p_t}^{p_b} \iint \frac{\partial(\omega k)}{\partial p} dsdp - \frac{1}{Sg} \int_{p_t}^{p_b} \iint \mathbf{V}_\psi \cdot \nabla_h \Phi dsdp - \\ \frac{1}{Sg} \int_{p_t}^{p_b} \iint \mathbf{V}_\chi \cdot \nabla_h \Phi dsdp &+ \text{RES} \end{aligned} \quad (3)$$

where  $S$  is the area of the cyclone's central region;  $P_b$  and  $P_t$  are the pressure at the bottom and top level of an air column;  $k$  is the horizontal KE;  $\mathbf{M}_h$  is the horizontal moving speed vector of the cyclone;  $\mathbf{V}_\psi$  and  $\mathbf{V}_\chi$  are the rotational and divergent wind vectors, respectively; and  $\Phi$  is geopotential. The first to the sixth terms on

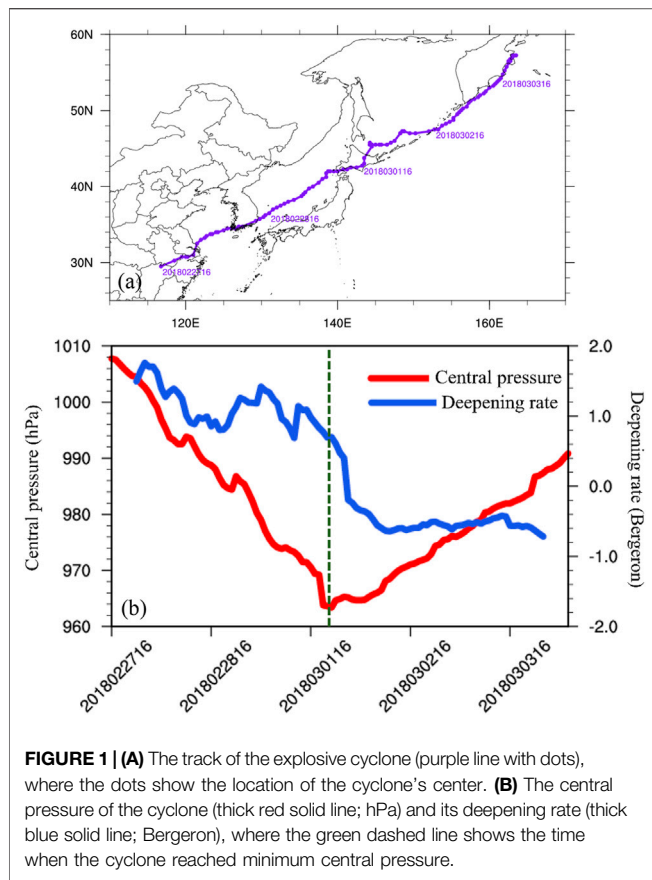


**FIGURE 1 | (A)** The track of the explosive cyclone (purple line with dots), where the dots show the location of the cyclone's center. **(B)** The central pressure of the cyclone (thick red solid line; hPa) and its deepening rate (thick blue solid line; Bergeron), where the green dashed line shows the time when the cyclone reached minimum central pressure.

the right-hand side of Eq. 3 denote the KE variations due to the cyclone's displacement (Term 1), the rotational wind's transport (Term 2), the divergent wind's transport (Term 3), the vertical transport (Term 4), the work on rotational wind by pressure gradient force (Term 5), and the work on divergent wind by pressure gradient force (Term 6), respectively. The term RES denotes the residual effects that were mainly due to friction, subgrid processes, and calculation errors.

In this study, the rotational/divergent wind was calculated by using the method developed by Cao and Xu (2011), which had been proven to be accurate and effective in generating rotational/divergent wind within a limited domain.

## OVERVIEW OF THE EVENT

During the period from February 27 to March 4, 2018, an extratropical cyclone appeared over the northwest Pacific Ocean (Figure 1A), which caused strong winds in its surrounding regions. This cyclone formed at 1600 UTC on February 27, around the junction of Anhui and Jiangxi provinces, moved in the northeast direction in its whole life span, and dissipated at 0600 UTC on March 4 (it lasted for ~110 h), around Kamchatka Peninsula. During this period, an upper-level jet was mainly located in the zonal band of 22–46°N (not shown), with a large-value zone exceeding  $100 \text{ m s}^{-1}$

stretching from East China to the central section of Japan. In the same period, a middle-tropospheric shortwave trough moved from East China to the central and southern sections of Japan along with the EEC (not shown), west of which a strong cold advection appeared. Along with the upper-level jet and the shortwave trough, a notable tropopause folding process appeared (not shown), which resulted in positive potential vorticity anomalies in the middle troposphere. These were favorable for the developing of the EEC (Fu et al., 2018). In this study, the evolutionary processes of this cyclone may be roughly divided into two stages: the first is from 1600 UTC on February 27 to 1800 UTC on March 1, during which the cyclone's central pressure lowered rapidly (Figure 1B); the second is from 1800 UTC on March 1 to 0600 UTC on March 4, during which the cyclone increased gradually in its central pressure. Therefore, the first stage is named the developing stage of the cyclone. In this stage, the mean DR and maximum DR of the cyclone were 1.25 and 1.81 Bergeron, respectively, both of which indicated that the cyclone was an EEC (Sanders and Gyakum, 1980).

During the cyclone's developing stage, corresponding to its decreasing central pressure (Figure 1A), the cyclonic vorticity and wind speed both enhanced notably (Figure 2). According to the cyclone's mean size during its developing stage, a  $10^\circ$  (latitude)  $\times$   $12^\circ$  (longitude) box (purple dashed boxes in Figure 2) was determined to focus on the central region of the cyclone. This box was defined as the central region of the cyclone. The calculations based on this central region were insensitive to relatively small changes ( $\pm 0.5^\circ$ ) to its each boundary line, which means that the selection of the central region was representative. Overall, the selection of the EEC's central region was consistent with the principles documented in Fu (2001): "It should be large enough to cover the cyclone thoroughly but small enough to exclude other undesirable disturbances from the area." The correlations between the central region averaged KE/vorticity and the cyclone's central pressure were  $-0.75/-0.83$ , implying that both KE and vorticity were effective indicators for the cyclone's rapid development.

## KINETIC ENERGY AND VORTICITY BUDGETS

### Kinetic Energy Budget

During the developing stage, the cyclone showed rapid enhancement of KE (i.e., wind speed) in the layer of 950–850 hPa (not shown); therefore, this layer was used to calculate Eq. 3:  $P_b = 950 \text{ hPa}$  and  $P_t = 850 \text{ hPa}$ . As the gray line in Figure 3A shows, the sum of Terms 1–6 was positive in the developing stage. This means that there was an overall favorable condition for enhancing the cyclone's wind speed. Of all the six terms in Eq. 3, Term 5 (i.e., the work on the rotational wind by pressure gradient force) made the largest contribution to the cyclone's increasing wind speed (Figure 3E). This was because: 1) centripetal pressure gradient force grew quickly as the central pressure of the cyclone lowered (Figure 2); 2) rotational wind was much larger than divergent wind (not shown); and (iii), the angle

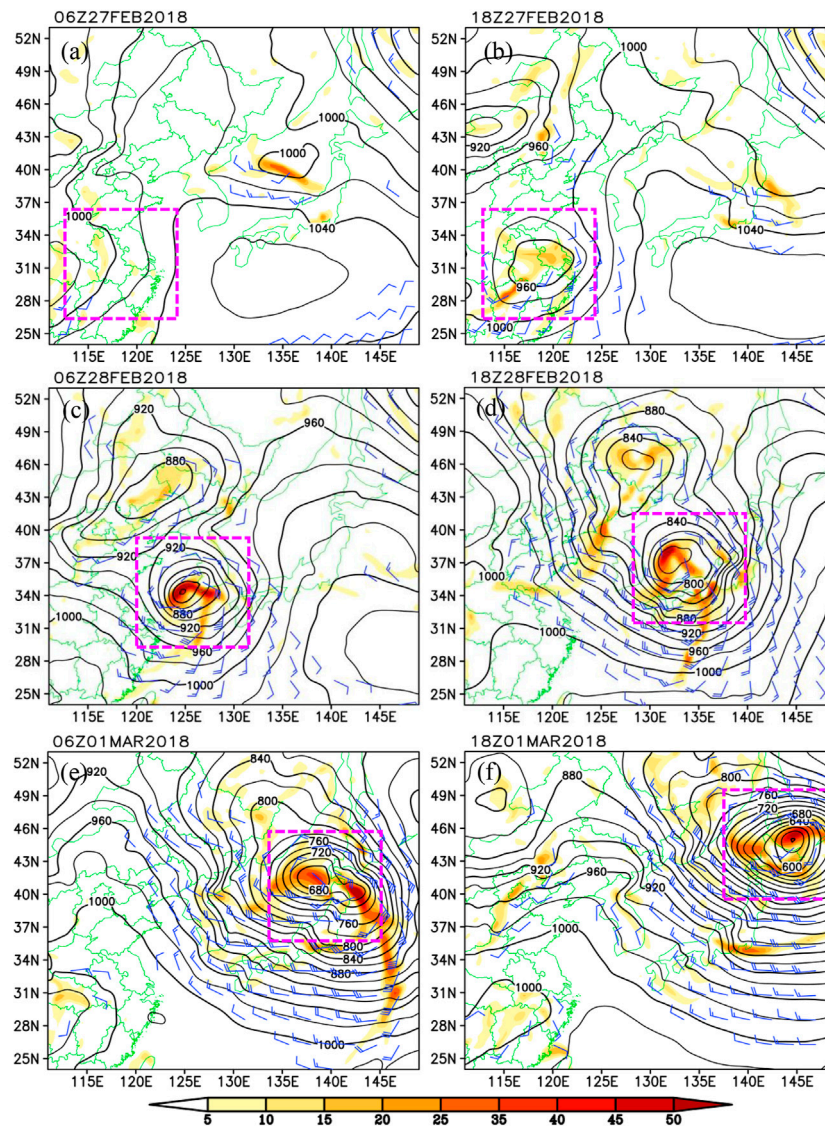


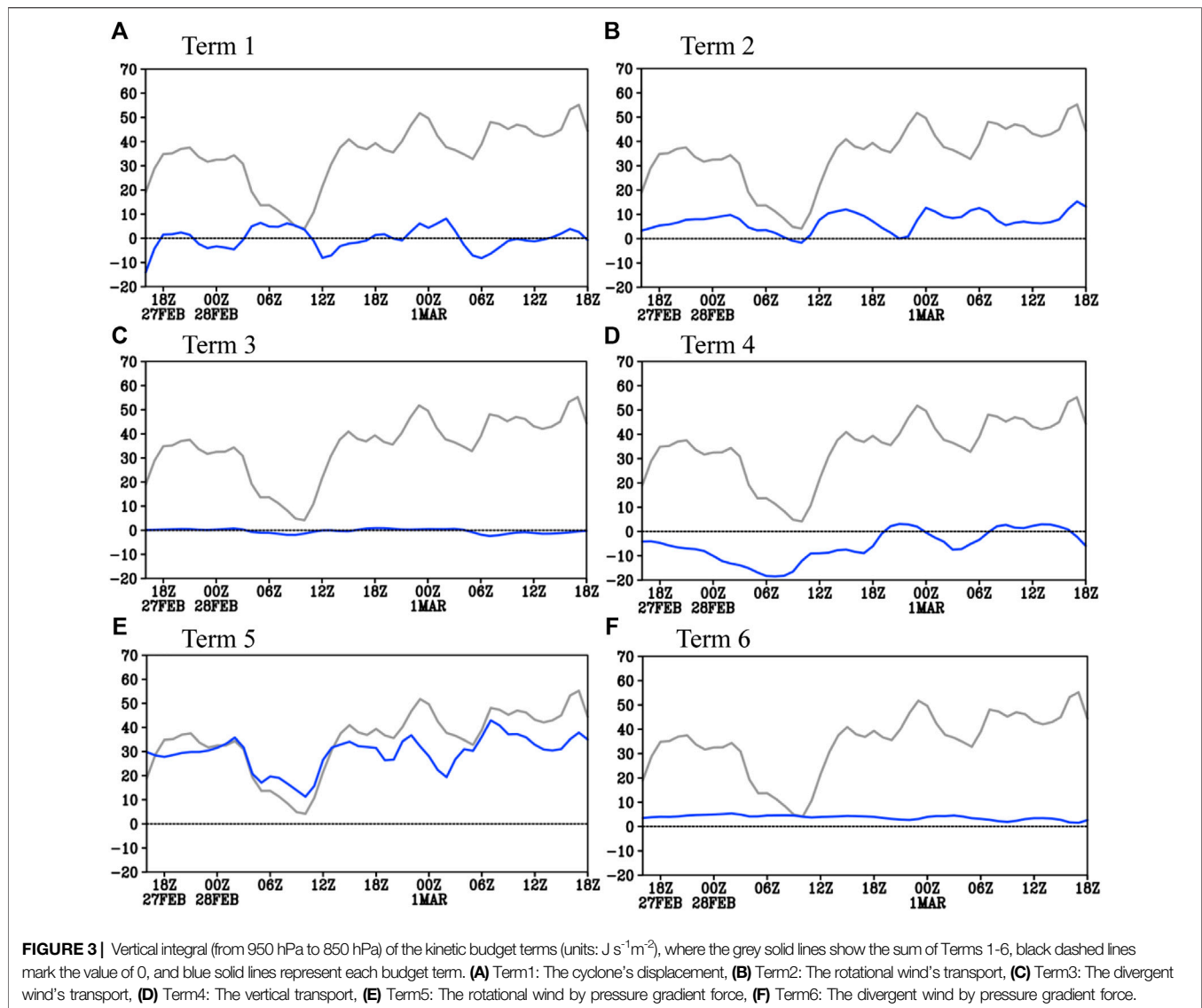
**FIGURE 2** | Geopotential height (black solid lines; gpm), wind above  $10 \text{ m s}^{-1}$  (blue wind bar; a full bar is  $10 \text{ m s}^{-1}$ ), and cyclonic vorticity (shading;  $10^{-5} \text{ s}^{-1}$ ) at 900 hPa at **(A)** 06 Z on February 27, 2018, **(B)** 18 Z on February 27, 2018, **(C)** 06 Z on February 28, 2018, **(D)** 18 Z on February 28, 2018, **(E)** 06 Z on March 1, 2018, **(F)** 18 Z on March 1, 2018, where the purple dashed boxes mark the central region of the explosive cyclone.

between rotational wind and the centripetal pressure gradient force was overall smaller than  $90^\circ$  (not shown). Term 2 (i.e., rotational wind's transport of KE) acted as the second dominant factor for the wind enhancement (**Figure 3B**). As **Figure 2** shows, the regions surrounding the cyclone's central region featured strong wind (i.e., KE was large). Overall, the rotational wind transported large KE centripetally (not shown). This resulted in net import of KE into the central region that enhanced the cyclone's wind speed. Term 6 (i.e., the work on the divergent wind by pressure gradient force) was also favorable, whereas its relative contribution was small (**Figure 3F**). Term 4 (vertical transport of KE) exerted the largest effect in decelerating the KE associated with the cyclone (**Figure 3D**). This was because the ascending motions (not shown) transported lower-level

strong KE upward, which resulted in a net export of KE from the lower troposphere. Term 1, which denoted the effect due to the cyclone's displacement, mainly decelerated the cyclone's development in wind speed (**Figure 3A**). This was because the cyclone mainly moved from regions with stronger KE to those with weaker KE (Fu and Sun, 2012). The KE features within the background environment affected the variation of EECs through this effect. Term 3 (divergent wind's transport of KE) showed a nearly neutral effect, as divergent wind was generally weak (not shown).

### Vorticity Budget

Corresponding to the rapid enhancement in KE, the cyclone's cyclonic vorticity also intensified quickly in the layer of



850–950 hPa, as term TOT (black lines in **Figure 4**) kept a large positive value in this layer. Among the four budget terms of **Eq. 2**, the convergence-associated STR (red lines in **Figure 4**) was the most favorable factor for the increase of the cyclone's cyclonic vorticity (strong lower-level convergence within the central region produced cyclonic vorticity through vertical stretching) during its developing stage. The second most favorable factor was the vertical transport of vorticity (blue lines in **Figure 4**) before 2000 UTC on February 28 (not shown), after that, the tilting effect (green line in **Figure 4D**) became the second most favorable factor for the cyclone's enhancement in cyclonic vorticity. The horizontal transport of vorticity (i.e., HAV) was the most detrimental factor for the cyclone's development (orange lines in **Figure 4**), as it kept transporting cyclonic vorticity out from the cyclone's central region. Overall, the temporal mean effect of STR and VAV were positive, whereas those of HAV and TIL were negative. Therefore, the former two terms

favored the cyclone's increase in cyclonic vorticity, whereas the latter two terms acted conversely. From **Figure 4**, it can also be found that, in the layer of 850–450 hPa, the dominant factor for enhancing the cyclonic vorticity within the central region was VAV, i.e., the vertical transport of cyclonic vorticity from lower levels (this cyclonic vorticity was produced in the level below 850 hPa through the convergence-related STR). In contrast, term STR showed an overall negative effect. This means that this cyclone showed a vertical stretching from the bottom up; divergence governed the layer of 850–450 hPa during the cyclone's developing stage.

It should be noted that the Zwack–Okossi vorticity budget developed by Zwack and Okossi (1986) was used in previous studies to understand the evolutionary mechanisms of the EECs (e.g., Yoshida and Asuma, 2004; Fu et al., 2018). Some of these studies found that a strong upper tropospheric positive absolute vorticity advection and a warm advection associated with an upper-level jet usually acted as the key factors for the EECs'

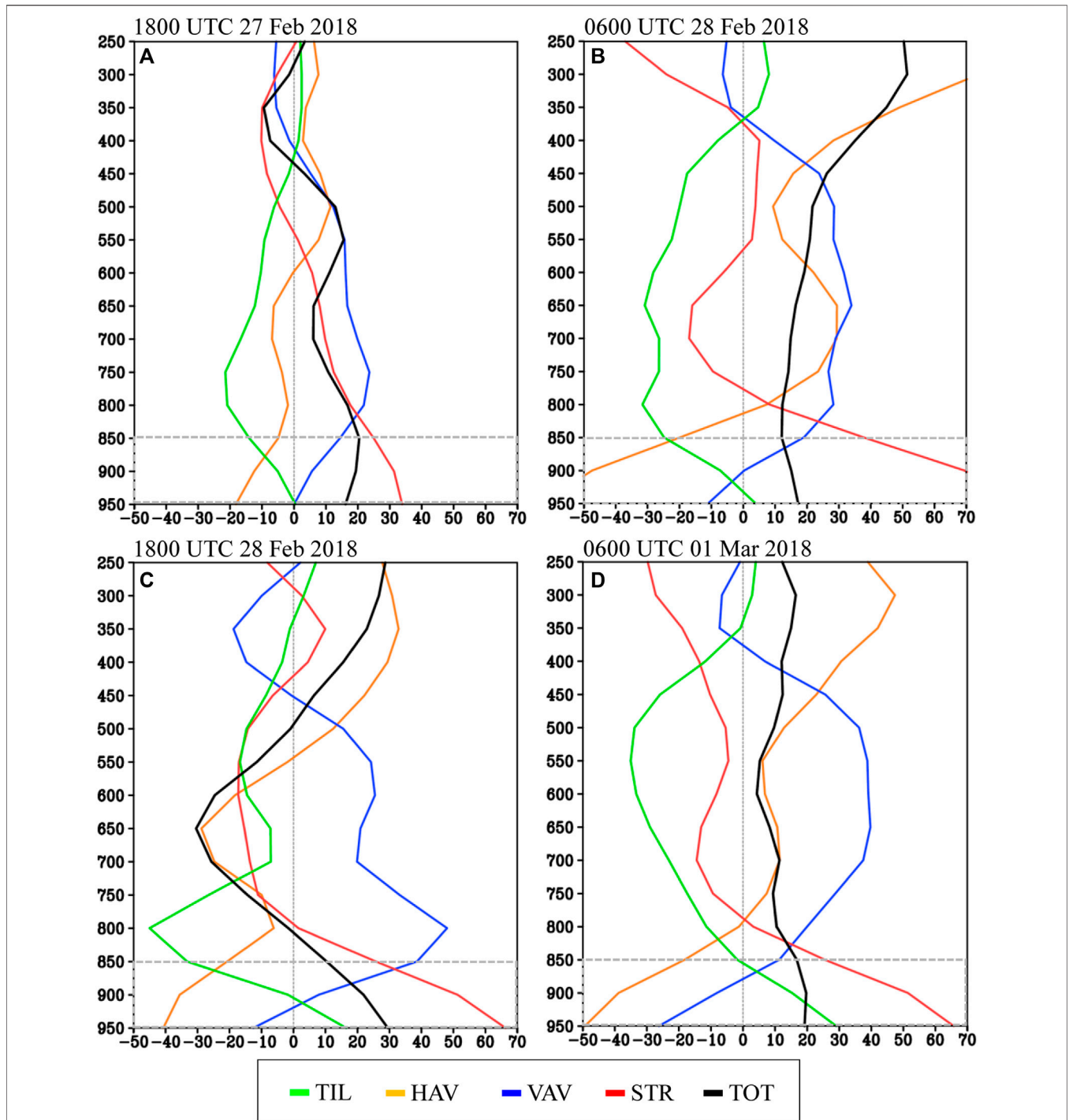


**FIGURE 4** | Central-region averaged vorticity budget terms ( $10^{-10}s^{-2}$ ) at typical stages, where the grey dashed lines mark the value of 0, and the grey dashed boxes outline the layer of 950–850 hPa. The green lines indicate the tilting effect, the orange lines indicate the horizontal advection of vorticity, the blue lines indicate the vertical advection of vorticity, the red lines indicate the stretching effect associated with divergence, and the black lines indicate the sum of TIL, HAV, VAV, STR, and APV.

development. The differences between the findings of these studies and the vorticity budget results in this study were mainly due to the following: 1) the Zwack–Okossi vorticity budget used the geostrophic vorticity instead of vorticity to

describe the variation of an EEC; and 2) the previous studies focused on the effects from the whole troposphere instead of only the lower troposphere (in this study we only focused on the lower layer).

## CONCLUSION AND DISCUSSION

In order to further the understanding of the mechanisms governing the rapid enhancement of EECs' rotation and wind speed during their developing stage, the vorticity and KE budgets were conducted on a typical EEC that appeared at the end of February 2018 over the Northwest Pacific Ocean. This cyclone lasted for ~110 h, and it was the strongest EEC that affected the coastal areas of China in the last 3 years. During its rapid development, its rotation and wind speed both strengthened quickly. The vorticity budget shows that the lower-level convergence-related vertical stretching (i.e., STR) was the most favorable factor for the increase of the cyclone's cyclonic vorticity; the second most favorable factor was the vertical transport of vorticity (i.e., VAV), which transported cyclonic vorticity upward (contributing to the upward extending of the cyclone). In contrast, the horizontal transport (i.e., HAV) caused a net export of cyclonic vorticity from the cyclone's central region, which made it the most detrimental factor for the cyclone's development. The KE budget indicates that the work on the rotational wind by the pressure gradient force made the largest contribution to the cyclone's increasing wind speed, and the net import transport of KE by the rotational wind acted as the second dominant factor. In contrast, the upward transport of KE exerted the largest effect in decelerating the KE associated with the EEC, and the effect due to the cyclone's displacement was the second most detrimental factor.

Overall, the enhancement of the EEC's rotation and wind speed was consistent with the deepening in its central pressure. A link between the rotation and the wind speed of an EEC is shown as follows: according to Green's theorem, the area-averaged vorticity within the EEC's central region equals the velocity circulation along the boundary line of the central region (Fu et al., 2017). Therefore, the enhancement in the cyclone's rotation (reflected by the central region averaged vorticity) means increase in velocity circulation; increase in velocity circulation means that

wind along the boundary line of an EEC's central region strengthens. In this event, as the rotational wind was the dominant component of the horizontal wind associated with the EEC, and the rotational wind was mainly along the central region's boundary line, the enhancement of the EEC's rotation was consistent with the intensification in its wind speed. It should be noted that, although this study shows some useful results for understanding the mechanisms dominating the rapid development of the rotation and wind speed associated with the EEC over the Northwest Pacific Ocean, it surely has limitations in representing the universal features of this type of cyclone. To analyze more EECs in the future, is an effective way to fully address the two scientific questions raised in the Introduction.

## DATA AVAILABILITY STATEMENT

Publicly available datasets were analyzed in this study. These data can be found here: <https://cds.climate.copernicus.eu/cdsapp#!/dataset/reanalysis-era5-single-levels?tab=overview>.

## AUTHOR CONTRIBUTIONS

HW and MD contributed to conception and design of the research. CS organized the database. BZ performed the statistical analysis. MD drew the figures. HW wrote the manuscript. All authors contributed to manuscript revision and read and approved the submitted version.

## FUNDING

This work was supported by the national key R&D Program of China (Grant Nos.2019YFC1510104).

## REFERENCES

- Bosart, L. F. (1981). The Presidents' Day Snowstorm of 18-19 February 1979: A Subsynoptic-Scale Event. *Mon. Wea. Rev.* 109, 1542–1566. doi:10.1175/1520-0493(1981)109<1542:tpdsof>2.0.co;2
- Cao, J., and Xu, Q. (2011). Computing Streamfunction and Velocity Potential in a Limited Domain of Arbitrary Shape. Part II: Numerical Methods and Test Experiments. *Adv. Atmos. Sci.* 28, 1445–1458. doi:10.1007/s00376-011-0186-5
- Chen, S.-J., and Dell'Osso, L. (1987). A Numerical Case Study of East Asian Coastal Cyclogenesis. *Mon. Wea. Rev.* 115, 477–487. doi:10.1175/1520-0493(1987)115<0477:ancsoe>2.0.co;2
- Chen, T.-C., Alpert, J. C., and Schlatter, T. W. (1978). The Effects of Divergent and Nondivergent Winds on the Kinetic Energy Budget of a Mid-latitude Cyclone: A Case Study. *Mon. Wea. Rev.* 106, 458–468. doi:10.1175/1520-0493(1978)106<0458:teodan>2.0.co;2
- Fu, G. (2001). *Polar Lows: Intense Cyclone in Winter*. Beijing, China: China Meteorological Press, 206.
- Fu, S.-M., Sun, J.-H., Li, W.-L., and Zhang, Y.-C. (2018). Investigating the Mechanisms Associated with the Evolutions of Twin Extratropical Cyclones over the Northwest Pacific Ocean in Mid-January 2011. *J. Geophys. Res. Atmos.* 123, 4088–4109. doi:10.1002/2017jd027852
- Fu, S.-M., Sun, J.-H., Luo, Y.-L., and Zhang, Y.-C. (2017). Formation of Long-Lived Summertime Mesoscale Vortices over Central East China: Semi-Idealized Simulations Based on a 14-Year Vortex Statistic. *J. Atmos. Sci.* 74, 3955–3979. doi:10.1175/jas-d-16-0328.1
- Fu, S.-M., Zhang, J.-P., Sun, J.-H., and Zhao, T.-B. (2016). Composite Analysis of Long-Lived Mesoscale Vortices over the Middle Reaches of the Yangtze River valley: Octant Features and Evolution Mechanisms. *J. Clim.* 29, 761–781. doi:10.1175/jcli-d-15-0175.1
- Fu, S., and Sun, J. (2012). Circulation and Eddy Kinetic Energy Budget Analyses on the Evolution of a Northeast China Cold Vortex (NCCV) in May 2010. *J. Meteorol. Soc. Jpn.* 90, 553–573. doi:10.2151/jmsj.2012-408
- Fu, S., Sun, J., and Sun, J. (2014). Accelerating Two-Stage Explosive Development of an Extratropical Cyclone over the Northwestern Pacific Ocean: a Piecewise Potential Vorticity Diagnosis. *Tellus* 66, 1–22. doi:10.3402/tellusa.v66.23210
- Fu, S., Sun, J., Zhao, S., and Li, W. (2011). The Energy Budget of a Southwest Vortex with Heavy Rainfall over South China. *Adv. Atmos. Sci.* 28, 709–724. doi:10.1007/s00376-010-0026-z
- Hersbach, H., Bell, B., Berrisford, P., Hirahara, S., Horányi, A., Muñoz-Sabater, J., et al. (2020). The ERA5 Global Reanalysis. *Q.J.R. Meteorol. Soc.* 146, 1999–2049. doi:10.1002/qj.3803
- Hirschberg, P. A., and Fritsch, J. M. (1991b). Tropopause Undulations and the Development of Extratropical Cyclones. Part II: Diagnostic Analysis and

- Conceptual Model. *Mon. Wea. Rev.* 119, 518–550. doi:10.1175/1520-0493(1991)119<0518:tuatdo>2.0.co;2
- Hirschberg, P. A., and Fritsch, J. M. (1991a). Tropopause Undulations and the Development of Extratropical Cyclones. Part I. Overview and Observations from a Cyclone Event. *Mon. Wea. Rev.* 119, 496–517. doi:10.1175/1520-0493(1991)119<0496:tuatdo>2.0.co;2
- Iwao, K., Inatsu, M., and Kimoto, M. (2012). Recent Changes in Explosively Developing Extratropical Cyclones over the winter Northwestern Pacific. *J. Clim.* 25, 7282–7296. doi:10.1175/jcli-d-11-00373.1
- Jia, Y., and Zhao, S. (1994). A Diagnostic Study of Explosive Development of Extratropical Cyclone over East Asia and West Pacific Ocean. *Adv. Atmos. Sci.* 11, 251–270.
- Jiang, L. Z., Fu, S. M., Sun, J. H., Fu, R., Li, W. L., Zhao, S. X., et al. (2021a). Surface Wind and Vertical Extent Features of the Explosive Cyclones in the Northern Hemisphere Based on the ERA-I Reanalysis Data. *Int. J. Climatol.* 42, 993–1014. doi:10.1002/joc.7284
- Jiang, L. Z., Yu, H., Dong, L., Fu, S. M., Sun, J. H., Zheng, F., et al. (2021b). On the Vertical Extending of the Explosive Extratropical Cyclone: A Case Study. *Atmos. Sci. Lett.* 2021, e1028. doi:10.1002/asl.1028
- Kirk, J. R. (2003). Comparing the Dynamical Development of Two Mesoscale Convective Vortices. *Mon. Wea. Rev.* 131, 862–890. doi:10.1175/1520-0493(2003)131<0862:ctddot>2.0.co;2
- Kuo, Y.-H., Low-Nam, S., and Reed, R. J. (1991). Effects of Surface Energy Fluxes during the Early Development and Rapid Intensification Stages of Seven Explosive Cyclones in the Western Atlantic. *Mon. Wea. Rev.* 119, 457–476. doi:10.1175/1520-0493(1991)119<0457:eosefd>2.0.co;2
- Lupo, A. R., Smith, P. J., and Zwack, P. (1992). A Diagnosis of the Explosive Development of Two Extratropical Cyclones. *Mon. Wea. Rev.* 120, 1490–1523. doi:10.1175/1520-0493(1992)120<1490:adoted>2.0.co;2
- Macdonald, B. C., and Reiter, E. R. (1988). Explosive Cyclogenesis over the Eastern United States. *Mon. Wea. Rev.* 116, 1568–1586. doi:10.1175/1520-0493(1988)116<1568:ecoteu>2.0.co;2
- Parsons, K. E., and Smith, P. J. (2004). An Investigation of Extratropical Cyclone Development Using a Scale-Separation Technique. *Mon. Wea. Rev.* 132, 956–974. doi:10.1175/1520-0493(2004)132<0956:aioecd>2.0.co;2
- Reed, R. J., and Albright, M. D. (1986). A Case Study of Explosive Cyclogenesis in the Eastern Pacific. *Mon. Wea. Rev.* 114, 2297–2319. doi:10.1175/1520-0493(1986)114<2297:acsoec>2.0.co;2
- Rossa, A. M., Wernli, H., and Davies, H. C. (2000). Growth and Decay of an Extratropical Cyclone's PV-Tower. *Meteorology Atmos. Phys.* 73, 139–156. doi:10.1007/s007030050070
- Sanders, F. (1986). Explosive Cyclogenesis in the West-Central North Atlantic Ocean, 1981–84. Part I: Composite Structure and Mean Behavior. *Mon. Wea. Rev.* 114, 1781–1794. doi:10.1175/1520-0493(1986)114<1781:ecitwc>2.0.co;2
- Sanders, F., and Gyakum, J. R. (1980). Synoptic-Dynamic Climatology of the "Bomb". *Mon. Wea. Rev.* 108, 1589–1606. doi:10.1175/1520-0493(1980)108<1589:sdcot>2.0.co;2
- Schultz, D. M., Winters, A. C., Colle, B. A., Davies, H. C., and Volkert, H. (2018). Extratropical Cyclones: A century of Research on Meteorology's Centerpiece. *Meteorol. Monogr.* 59, 1610–1656. doi:10.1175/AMSMONOGRAPHIS-D-18-0015.1
- Smith, P. J., and Tsou, C.-H. (1988). Static Stability Variations during the Development of an Intense Extratropical Cyclone. *Mon. Wea. Rev.* 116, 1245–1250. doi:10.1175/1520-0493(1988)116<1245:ssvtdt>2.0.co;2
- Uccellini, L. W., Kocin, P. J., Petersen, R. A., Wash, C. H., and Brill, K. F. (1984). The Presidents' Day Cyclone of 18–19 February 1979: Synoptic Overview and Analysis of the Subtropical Jet Streak Influencing the Pre-cyclogenetic Period. *Mon. Wea. Rev.* 112, 31–55. doi:10.1175/1520-0493(1984)112<0031:tpdcotf>2.0.co;2
- Uccellini, L. W., and Kocin, P. J. (1987). The Interaction of Jet Streak Circulations during Heavy Snow Events along the East Coast of the United States. *Weather Forecast.* 2, 289–308. doi:10.1175/1520-0434(1987)002<0289:tiojcs>2.0.co;2
- Wang, S., Fu, G., and Pang, H. (2017). Structure Analyses of the Explosive Extratropical Cyclone: A Case Study over the Northwestern Pacific in March 2007. *J. Ocean Univ. China* 16, 933–944. doi:10.1007/s11802-017-3287-7
- Yoshida, A., and Asuma, Y. (2004). Structures and Environment of Explosively Developing Extratropical Cyclones in the Northwestern Pacific Region. *Mon. Wea. Rev.* 132, 1121–1142. doi:10.1175/1520-0493(2004)132<1121:saesod>2.0.co;2
- Zwack, P., and Okossi, B. (1986). A New Method for Solving the Quasi-Geostrophic omega Equation by Incorporating Surface Pressure Tendency Data. *Mon. Wea. Rev.* 114, 655–666. doi:10.1175/1520-0493(1986)114<0655:anmfst>2.0.co;2

**Conflict of Interest:** The authors declare that the research was conducted in the absence of any commercial or financial relationships that could be construed as a potential conflict of interest.

**Publisher's Note:** All claims expressed in this article are solely those of the authors and do not necessarily represent those of their affiliated organizations, or those of the publisher, the editors and the reviewers. Any product that may be evaluated in this article, or claim that may be made by its manufacturer, is not guaranteed or endorsed by the publisher.

Copyright © 2022 Wang, Du, Sun and Zhang. This is an open-access article distributed under the terms of the Creative Commons Attribution License (CC BY). The use, distribution or reproduction in other forums is permitted, provided the original author(s) and the copyright owner(s) are credited and that the original publication in this journal is cited, in accordance with accepted academic practice. No use, distribution or reproduction is permitted which does not comply with these terms.